RSC Mechanochemistry

ROYAL SOCIETY OF CHEMISTRY

PAPER

View Article Online
View Journal

Cite this: DOI: 10.1039/d5mr00152h

Mechanochemical synthesis of Cr_3C_2: investigating the role of pressure and temperature

Meet Koshiya[a] and Özgül Agbaba *[ab]

Chromium carbide (Cr_3C_2) is valued for its outstanding chemical stability, oxidation resistance, hardness, and thermal durability, making it essential for protective coatings, cutting tools, and wear-resistant components. Conventional Cr_3C_2 synthesis typically requires high temperatures and reducing atmospheres, leading to high energy consumption and significant equipment wear. Recently, we demonstrated that mechanochemical synthesis provides a more energy-efficient route, producing Cr_3C_2 with enhanced electrical conductivity and enabling its use in high-tech applications such as conductive fillers for fuel-cell electrodes. However, achieving single-phase Cr_3C_2 by ball milling remains challenging due to incomplete reaction and mixed-carbide formation, often requiring a subsequent annealing step at ~800 °C. In this study, we systematically investigate the influence of applied pressure and temperature on the mechanochemical formation of Cr_3C_2 to optimize phase purity and electrical performance. We show that increasing pressure significantly enhances phase selectivity, yielding Cr_3C_2 with superior conductivity and eliminating the need for post-annealing. This work establishes pressure-assisted mechanochemistry as an efficient and scalable pathway for producing high-purity Cr_3C_2 for advanced energy and coating applications.

Received 9th December 2025
Accepted 22nd March 2026

DOI: 10.1039/d5mr00152h

rsc.li/RSCMechanochem

Introduction

Chromium carbides (notably Cr_3C_2, Cr_7C_3, and $Cr_{23}C_6$) are well-established materials valued for their exceptional hardness, electrical conductivity, corrosion resistance, and thermal stability, making them indispensable in protective coatings, cutting tools, and wear-resistant components.[1,2] Traditionally, Cr_3C_2 is produced *via* high-temperature solid-state routes, most commonly through carbothermal reduction of chromium oxides or direct carburization of metallic chromium powders.[3–15] These processes typically require temperatures exceeding 1400 °C and strongly reducing atmospheres such as H_2/CH_4 mixtures to ensure complete carbide formation.

Although state-of-the-art at industrial scale, such synthesis routes remain highly energy-intensive and impose severe chemical and mechanical stress on processing equipment due to the corrosive and reducing environments. The reliance on combustible gas mixtures also introduces safety risks, while the formation of CO and CO_2 as by-products raises environmental concerns. Furthermore, prolonged reaction times and high thermal budgets provide limited control over phase selectivity and particle morphology, often resulting in materials with heterogeneous structure and properties. Consequently, despite their technological importance, conventional production methods for Cr_3C_2 are costly, environmentally burdensome, and operationally challenging, motivating the search for alternative, lower-temperature synthesis strategies.

In response to such limitations of conventional thermal preparation routes, mechanochemistry has emerged as an attractive, energy-efficient alternative for the synthesis of various advanced materials, including transition metal carbides.[16,17] In addition, mechanochemical approaches have also been employed for the synthesis of alkaline carbides by ball milling, demonstrating the broader applicability of this technique for carbide formation.[18] This technique, which relies on mechanical energy to induce chemical transformations, enables reactions to occur at room temperature[19] and under solvent-free, environmentally friendly conditions.[10] Recent advances in mechanochemical synthesis have demonstrated its applicability to Cr_3C_2, revealing a promising route to produce this material at considerably lower temperatures and shorter timescales than conventional processes.[20–22] Furthermore, the mechanochemical synthesis, consisting of ball milling the metal chromium powder with a carbon source, enables the formation of nanostructured Cr_3C_2 with high electrical conductivity and excellent corrosion resistance. When used as a filler in coatings for metallic bipolar plates, Cr_3C_2 produced by high-energy ball milling under an argon atmosphere achieved conductivities exceeding 10^6 Sm^{-1} and interfacial contact resistance below 10 mΩ cm^2, significantly outperforming conventionally prepared commercial Cr_3C_2 due to the absence of thick surface oxides and improved particle purity.[23] Similar

[a]Department of Heterogeneous Catalysis, Max-Planck-Institut für Kohlenforschung, Mülheim an der Ruhr, 45470, Germany. E-mail: agbaba@mpi-muelheim.mpg.de
[b]MechSyn GmbH, Mülheim an der Ruhr, 45470, Germany

findings have been reported in earlier mechanochemical studies, where extended milling promoted the formation of nanocrystalline or amorphous chromium carbide phases (Cr_7C_3, $Cr_{23}C_6$) that can be converted to single phase Cr_3C_2 by post-annealing. The final phase composition and particle size are notably very sensitive to milling time, atmosphere, and stoichiometry.[24,25]

Despite the advantages of the mechanochemical route, challenges persist in achieving the pure Cr_3C_2 phase directly through ball milling. Incomplete reaction pathways and the formation of different chromium carbide compositions or oxide phases often necessitate a post-milling thermal treatment, typically around 800 °C under argon atmospheres, to achieve the desired single-phase product.[23]

Importantly, *in situ* studies have shown that both pressure and temperature exert a significant influence on mechanochemical reaction pathways and phase selectivity.[26,27] For chromium carbide, these parameters are particularly critical, as the Cr–C system exhibits a complex phase behavior with multiple stable and metastable carbide phases depending on the synthetic conditions.[24,28] In this work, we report a systematic study comparing the effects of elevated pressure and temperature on the mechanochemical synthesis of Cr_3C_2. Using a planetary ball mill and a shaker mill, we synthesized Cr_3C_2 particles under controlled inert atmosphere and characterized their phase composition, morphology, and electrical conductivity. By clarifying the roles of pressure and temperature, our work not only enables the optimized synthesis of high-purity Cr_3C_2 but also offers insights for the design of new mechanochemical material synthesis strategies.

Experimental

Mechanochemical synthesis of Cr_3C_2 particles

Chromium powder (particle size 45 μm, 99.99% purity, supplied by Sigma Aldrich) and graphite powder (particle size 5.1 μm, 99.2% purity, supplied by AMG Graphite) were used as starting materials for the synthesis of chromium carbide. The powders were weighed to achieve a Cr : C molar ratio of 3 : 2, following the stoichiometry required for the formation of Cr_3C_2 phase. The ball-to-powder weight ratio was maintained at 13 : 1, and zirconia (ZrO_2) balls in 10 mm diameter were used as the milling media. All powder handling, including mixing and loading, was performed in a glove box under a high-purity argon atmosphere (99.99%), with oxygen and water concentrations below 1 ppm to prevent oxidation and contamination. The appropriate proportions of chromium and graphite powders were introduced into milling vials and sealed within the glove box. Mechanochemical experiments were performed using three different mills: shaker mill experiments were carried out on a Retsch MM400 equipped with a custom-built 25 mL zirconia jar and a continuous argon gas flow system for 6–9 hours at room temperature (RT), 100 °C and 175 °C under atmospheric pressure with a fixed frequency of 25 Hz.[29] Planetary milling was conducted on a Fritsch Pulverisette 6 with a custom-built 130 mL stainless steel jar for 32 and 64 hours under argon pressures between 1 and 75 bar under room temperature at a fixed rotation speed of 550 rpm. High-energy ball milling was performed on a Retsch E_{max} with a 50 mL zirconia jar at 1000 rpm for 6 hours following the parameters reported in the ref. 23 Upon completion, the resulting powders were retrieved for further characterization and analysis. The experimental conditions for each sample, including mill type, milling duration, applied pressure, and temperature, are summarized in Table 1. This matrix of parameters was designed to identify the optimal milling conditions for promoting Cr_3C_2 formation while minimizing unreacted metallic chromium and contamination from the milling media.

Structural characterization of Cr_3C_2 particles

Powder X-ray diffraction (XRD) patterns for a qualitative phase analysis were obtained using a STOW theta/2theta diffractometer in Bragg–Brentano geometry with Cu $K_{\alpha 1,2}$ radiation at room temperature. Data were collected in the range of 20 to 90° with a step width of 0.05° 2θ and a counting time per step of 5 s using a pin diode detector (STOE & Cie GmbH). The recorded patterns were evaluated by comparison with entries in the ICDD PDF-2 database. Nitrogen physisorption measurements were performed on a Nova 3200e Surface Area & Pore Size Analyzer from Quantachrome Instruments at 77 K. Prior to the measurements, the samples were degassed at 150 °C for 24 h under vacuum. Specific surface areas (S_{BET}) were calculated using the Brunauer–Emmett–Teller (BET) method in the pressure range p/p_0 of 0.05–0.3.

Elemental composition was determined by energy-dispersive X-ray (EDX) bulk analysis using a Hitachi TM3030. Ultrahigh resolution scanning electron microscope (HR-SEM) micrographs were taken using a Hitachi S-5500 equipped with an energy-dispersive X-ray (EDX) spectrometer (Oxford Instruments) and a cold cathode field emission gun with a maximum acceleration voltage of 30 kV. All samples were prepared by sprinkling dried powder onto a Lacey Cu film supported by a Cu grid.

X-Ray photoelectron spectroscopy (XPS) measurements were performed on a custom spectrometer from SPECS GmbH, equipped with a Phoibos hemispherical energy analyzer and a 1D-DLD detector. The monochromatic Al-Kα X-ray radiation source ($E = 1486.6$ eV) was operated at 15 kV and 200 W. Survey scans were performed at 50 eV, while high-resolution scans were carried out at 20 eV. The medium area mode was used as the lens mode. During the experiment, the base pressure in the analysis chamber was maintained at 3 10^{-9} mbar. The fitting of the measured data was done using the CasaXPS software.[30]

Interfacial contact resistance

Powder conductivity measurements were performed using a custom-built four-point probe setup equipped with gold electrodes. Approximately 2 g of powder was transferred into a glass tube mounted on the bottom electrode, which was connected to a digital millimetre interfaced with data acquisition software. A second gold electrode was placed on top of the powder and connected to a movable rod capable of applying controlled compaction pressure. Measurements were carried

Table 1 Overview of the synthesis of chromium carbide under various milling conditions, including different milling types, milling durations, pressures, and temperatures

Sample ID	Mill type	Time (h)	Pressure (bar)	Temperature (°C)
S1	Shaker mill	6	—	RT
S2	Shaker mill	6	—	100
S3	Shaker mill	6	—	175
S4	Shaker mill	9	—	RT
S5	Shaker mill	9	—	100
S6	Shaker mill	9	—	175
S7	Planetary mill	32	—	RT
S8	Planetary mill	48	—	RT
S9	Planetary mill	64	—	RT
S10	Planetary mill	32	10	RT
S11	Planetary mill	32	20	RT
S12	Planetary mill	32	30	RT
S13	Planetary mill	32	75	RT
S14	Planetary mill	48	10	RT
S15	Planetary mill	48	20	RT
S16	Planetary mill	48	30	RT
S17[a]	High energy ball mill	6	—	RT

[a] The sample was post annealed at 800 °C under Argon atmosphere for two hours.

out at increasing pressures up to 8 bar. The resistance was recorded for the top, bottom and total contact points. A careful release of pressure from the top was ensured to avoid unequal distribution of pressure. The specific contact resistance ($\Omega\ cm^2$) was determined by normalizing the measured resistance to the electrode contact area. The data were exported and analysed to evaluate the effect of compaction pressure on powder conductivity.

Results and discussion

Thermal treatment experiments

To understand the possible influence of temperature on the Cr_3C_2 synthesis, tests were conducted utilizing a shaker mill with regulated external heating. The X-ray diffraction patterns of powders S1–S6 milled under various milling temperatures and durations are presented in Fig. 1. Initial experiments at room temperature (samples S1 and S4) show only partial formation of Cr_3C_2, with no complete phase transformation even after extending the milling time from 6 to 9 hours. The XRD patterns reveal strong reflections of unreacted chromium and only minor indications of Cr_3C_2 formation. Increasing the milling duration has little effect on peak intensities, while zirconia impurities from the milling media became more pronounced.

Temperature-assisted experiments were carried out at 100 °C (S2) and 175 °C (S3) for 6 hours. By tracking the peak intensities at 35°, 39°, and 50°, the XRD patterns revealed a slight improvement in the conversion to Cr_3C_2 compared to those milled at room temperature. However, despite the higher peak intensities, complete conversion was still not achieved, and substantial amounts of unreacted chromium persisted. This incremental improvement confirms that increasing temperature facilitates the reaction and promotes Cr_3C_2 formation, most likely by providing additional thermal energy to overcome kinetic barriers. Nonetheless, the persistence of unreacted starting material indicates that the applied reaction conditions were still suboptimal. To further enhance the reaction, the milling time was extended. Additional experiments were conducted at 100 °C (S5) and 175 °C (S6) for 9 hours. Both experiments showed only marginal additional changes in the crystallinity of the product and incomplete conversion to Cr_3C_2 compared to their 6 hours counterparts. Moreover, the impurity level increased notably in the longer-milled powders, suggesting that extended processing increases zirconia contamination from the milling media.

Increasing the external temperature enhances the energy of the milling system, raising local temperatures that promote atomic diffusion and bond formation. Although mechanical activation lowers the required synthesis temperature,[16,19] the

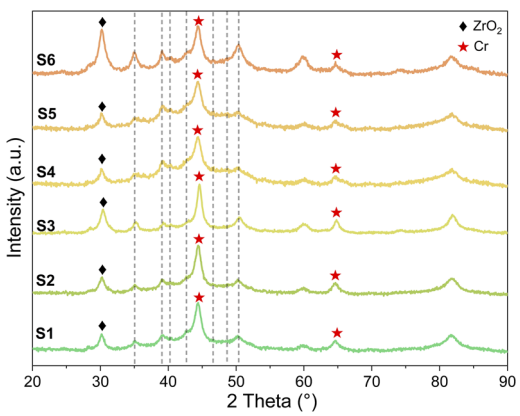

Fig. 1 X-ray diffraction patterns of powders S1–S6 milled under various milling temperatures and durations using a shaker mill. The reference diffraction peaks of the Cr_3C_2 phase (PDF 00-035-0804) are marked by dashed lines, unreacted chromium is indicated by red stars, and zirconia impurities originating from the milling media are marked by black diamonds.

100–175 °C range used here insufficient for complete solid state diffusion and reaction in the Cr–C system. Milling at elevated temperatures presents technical challenges, as the system cannot be safely operated above 200 °C and requires carful manual control to maintain stable conditions.

Ultimately, one of the main advantages of mechanochemistry lay in performing reactions efficiently at room temperature. Therefore, optimizing other parameters, such as the type of the milling device, duration, or applied pressure, was considered a more viable strategy. Based on these findings, subsequent experiments were carried out using a planetary mill under varying milling durations and pressures.

Effect of milling time

Fig. 2 shows the XRD patterns of samples milled in a planetary mill without the application of external pressure or heat. The powders were milled for varying durations of 32, 48, and 64 hours. Despite these extended milling times, the XRD patterns of all three samples exhibited only reflections corresponding to metallic chromium, with no detectable peaks of the desired Cr_3C_2 phase. This indicates that even prolonged milling, up to 64 hours at the highest possible speed, did not provide sufficient mechanical energy under these conditions to overcome the activation energy barrier required for chromium carbide formation. The type and amount of energy applied during mechanochemical milling is known to be dependent on the mill's mechanical design and the geometry of the grinding vessel; shaker and planetary mills deliver different energy doses, in this case, the shaker mill (with moderate heating) achieved measurable Cr_3C_2 formation within 6–9 h, while the planetary mill at room temperature showed only Cr reflections even after 64 h.

Pressure-induced experiments

To further enhance the energy input and investigate its impact on phase formation, experiments were conducted in a planetary mill under varying external pressures. Fig. 3 presents the XRD patterns of obtained samples after 32 h of milling under various pressure conditions. Pressurized experiments conducted with an applied pressure of 10 bar demonstrated the formation of Cr_3C_2 (S10). Compared to milling experiments performed without additional applied pressure, these conditions promoted more significant phase conversion, resulting in sharper and more defined Cr_3C_2 reflections.

However, a minor amount of the Cr_7C_3 phase was also detected, suggesting that complete phase purity was not achieved. The applied pressure was incrementally increased to 20 bar, 30 bar and subsequently up to 75 bar to optimize reaction conditions and enhance the formation of Cr_3C_2 phase (Fig. 3 and S11–S13). While higher pressure increased the intimate contact between reactants and particle diffusion, enhancing the mechanical impact energy for phase transformation, the XRD pattern revealed a more complex outcome. These peaks became progressively stronger and more prominent with increasing pressure, alongside the desired Cr_3C_2 phase.

The effect of pressure on phase formation can be attributed to its influence on particle contact and diffusion kinetics during milling. Applying external pressure enhances interparticle bonding by promoting plastic deformation and reducing the distance between metal and carbon particles. This facilitates more effective mechanical mixing and increases the number of active contact points where diffusion can occur. At the same time, the compressed environment shortens the distance atoms need to move for carbide formation, making the reaction proceed more quickly.[26] Jiang *et al.* reported that increased pressure during the high-pressure sintering of Cr_3C_2 accelerates the plastic and elastic deformation of particles that closes pores and brings grains into intimate contact. This close contact promotes viscous flow and vacancy transport along grain boundaries, strengthening intergranular bonding and accelerating atomic diffusion. And lowers the temperature required for diffusion and bonding.[26,31] In the present work, the applied pressure likely provided comparable benefits, improving local contact and diffusion dynamics and thereby lowering the

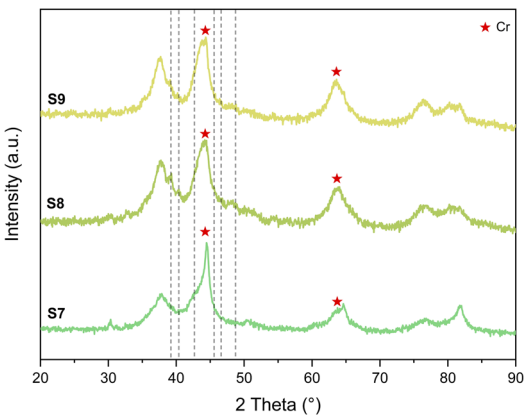

Fig. 2 X-ray diffraction patterns of powders S7, S8, and S9 milled for 32, 48, and 64 hours, respectively, *via* planetary mill. The diffraction peak positions for the Cr_3C_2 phase (PDF 00-035-0804) are indicated by dashed lines.

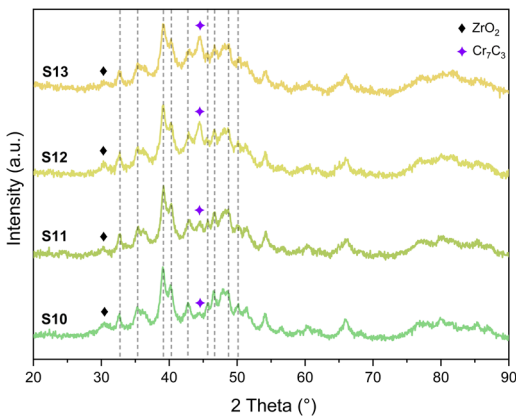

Fig. 3 X-Ray diffraction patterns of samples S10, S11, S12, and S13. The samples were milled for 32 hours under 10, 20, 30, and 75 bar pressures, respectively, *via* planetary mill. The referenced diffraction peaks of the Cr_3C_2 phase (PDF 00-035-0804) are marked by grey dashed lines, while those corresponding to the Cr_7C_3 phase (PDF 00-036-1482) are indicated by purple symbols.

activation barrier for the Cr–C reaction and enabling chemical pathways that are inaccessible under ambient conditions.

Furthermore, the milling duration was extended to 48 hours to investigate its effect on phase formation. A notable improvement in phase purity was observed in the samples milled at 10 bar. In contrast, the samples milled at 20 bar showed minimal changes in phase composition, with an increase in crystallinity. The absence of other chromium carbide reflections under these conditions after 48 hours suggests that these provide a favorable environment for the selective formation and stabilization of the Cr_3C_2 phase. Rietveld refinement of the corresponding XRD pattern obtained under the optimized milling conditions (48 h, 20 bar) indicates the formation of Cr_3C_2 as the dominant phase with a refined phase fraction of approximately 99% (Fig. S4), confirming the high conversion efficiency of the mechanochemical process. This indicates that enough collision and impact were applied over a longer duration to get the desired product while avoiding the formation of undesired by products.

At 30 bar (S16), a small peak of the Cr_7C_3 phase was observed (Fig. 4). This observation aligns with the trend seen in the 32 hours experiments, where increasing pressure led to the formation of various carbide phases. These results strongly suggest that while pressure can promote faster reactions, it can also alter the formation pathways of different carbide phases. At higher pressures, the increased particle contact within the milling environment may enable the formation of additional chromium carbide phases (Cr_7C_3, $Cr_{23}C_6$), which are less stable under these specific conditions.

Properties of mechanochemically synthesized chromium carbide

The particle size distribution and morphology are given in Fig. 5. The particles exhibit an agglomerated structure with an irregular shape and a relatively narrow size distribution from below 100 nanometers to several hundred nanometres. This agglomeration can be attributed to the mechanism of high-energy milling. During the initial stage, the impact forces deform the particles, leading to work hardening and fracture. Newly formed surfaces promote cold welding, which contributes to particle agglomeration. As milling progresses, repeated deformation induces further work hardening, followed by fracture through fatigue failure or fragmentation of loosely bonded structures. The fragments produced can lead to a reduction in particle size.[32]

A clear effect of milling pressure is observed when comparing samples S13 and S15. The higher pressure shows porous agglomerates consisting of fine, angular primary particles, suggesting excessive fracturing and cold welding due to strong mechanical impacts. In contrast, sample S15 has a denser and more compact morphology with smoother boundaries between particles. The lower impact energy at this pressure promotes deformation and welding over fragmentation, producing more consolidated aggregates.[33,34] The annealed sample (S17) exhibits the most pronounced morphological transformation. The fine agglomerates formed during milling coalesce into larger, dense grains with smooth, rounded surfaces. This change results from thermal sintering, when atomic diffusion reduces surface energy, eliminating pores and promoting grain growth.[35,36] The agglomeration of the carbide particles, which is reflected in the relatively high specific surface area of 25–35 $m^2\ g^{-1}$ for most samples, is promoted by the high impact energy of the ball milling process. In contrast, the annealed sample S17 exhibits a significantly lower surface area of 4 $m^2\ g^{-1}$. The elemental analysis revealed contamination levels in the carbides of 2–6 wt% Zr and 0.1–3 wt% Fe. The relatively high Zr content is likely associated with the extended milling duration, the hardness of the metal, and the limited amount of graphite present in the jar, which acts as a lubricant.

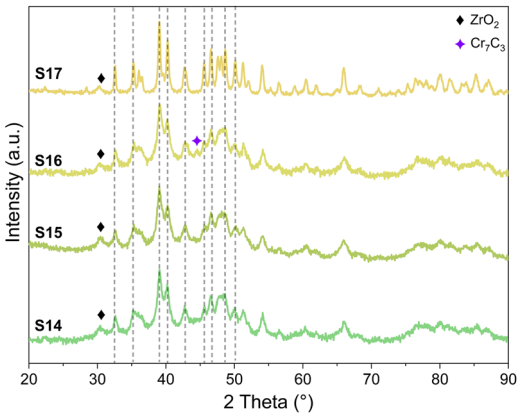

Fig. 4 X-Ray diffraction patterns of samples S14, S15, and S16. The samples were milled for 48 hours under 10, 20, and 30 bar pressures, respectively, *via* planetary mill, while sample S17 was milled using the High Energy Ball Mill (E_{max}) for 6 hours and annealed at 800 °C for 2 h. The diffraction peak positions for the Cr_3C_2 phase (PDF No. 00-035-0804) are indicated by grey dashed lines.

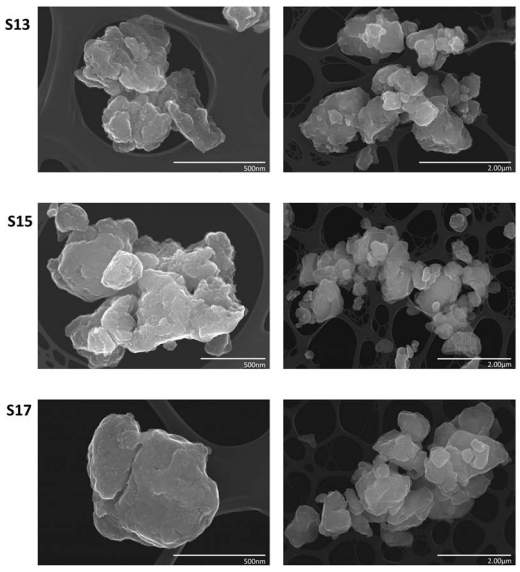

Fig. 5 High-resolution SEM images of the synthesized chromium carbides samples S13, S15 and S17. The samples S13 was milled for 32 h at 75 bar, S15 for 48 h at 20 bar, and S17 was milled in the E_{max} mill under ambient conditions followed by annealing.

Interfacial contact resistance measurement

Fig. 6 shows the dependence of specific contact resistance on compaction pressure for three different samples. In all cases, the resistance decreases with increasing pressure, which reflects the improved particle–particle contact and reduction of interfacial voids during compaction. However, the absolute resistance values differ significantly depending on the synthesis conditions.

Sample S17 (red curve in Fig. 6) shows the lowest contact resistance, consistent with the expected high phase purity and enhanced conductivity after ballmilling and annealing. Interestingly, sample S15 exhibits a nearly identical resistance. This indicates that longer durations of planetary milling at 20 bar can suppress the formation of secondary phases, yielding conductivity comparable to that of the annealed Cr_2C_3 without requiring an additional heat-treatment step.

In contrast, sample S13 (green curve) milled under 75 bars pressure, which exhibits a much higher contact resistance across the entire range. This large difference implies that the corresponding sample possesses inferior conductivity, most likely due to the formation of unnecessary secondary phases, which are more insulating or covalent in character.[37] A less conductive phase would increase the interfacial barrier to charge transport, thereby raising the overall resistance.[38,39]

To understand these differences, X-ray photoelectron spectroscopy (XPS) was performed on all three samples (Fig. 7). The spectra reveal that samples S15 and S17 have similar carbide-to-oxide ratios on their surfaces, consistent with their comparable conductivity. In contrast, sample S13, which exhibits low electrical conductivity, displays a substantially higher oxide signal, indicating the presence of a thicker surface oxide layer. This observation parallels reports on commercial Cr_3C_2 powders, where a thick, non-conducting oxide layer was found to lower conductivity. The conventional methods of carbide synthesis uses reducing gas mixture at high temperature, but oxygen is not fully excluded, and some routes start from oxides.[13–15] sThis could lead to oxide formation/retention, which would affect the electrical properties. However, a small oxide signal was also detected on the mechanochemically synthesised Cr_3C_2 samples, which may result from exposure of the precursors to oxygen prior to synthesis or from scratching out the milling jars in air. The results demonstrate that minimizing oxide formation during synthesis and handling is critical for achieving high electrical conductivity and that mechanochemical synthesis under controlled atmospheres can produce powders with favorable surface characteristics.

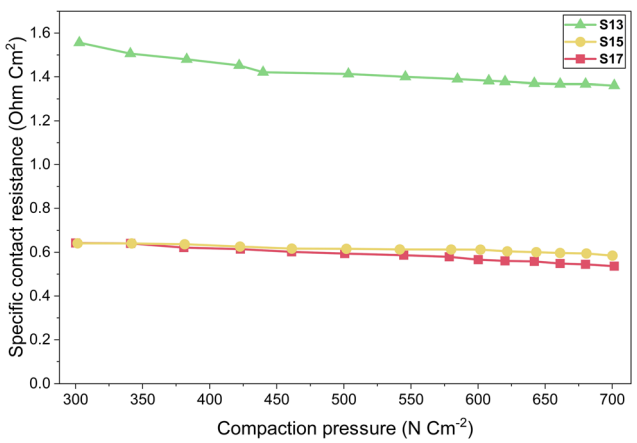

Fig. 6 Specific contact resistance of the powders as a function of compaction pressure.

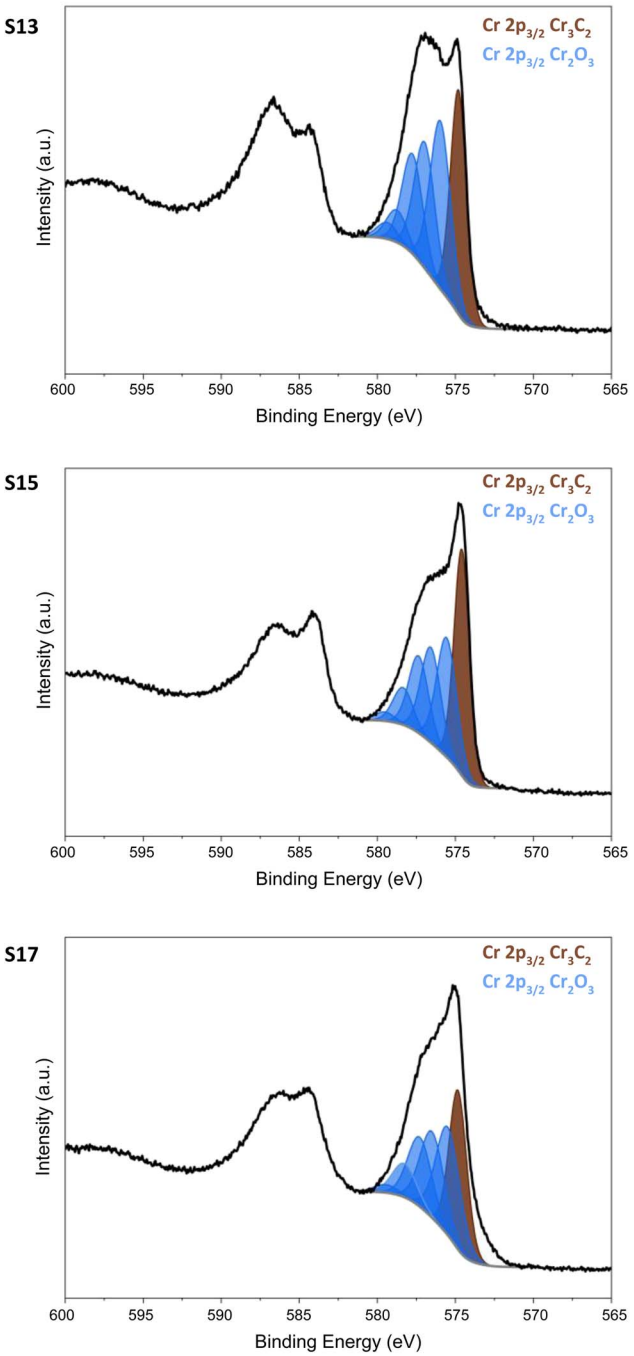

Fig. 7 XPS spectra of the Cr 2p region of samples S13, S15, and S17. The signal at about 574 eV is attributed to Cr_3C_2, and 577 eV attributed to oxidized chromium multiplet species.

Conclusions

This study demonstrates that the mechanochemical synthesis of Cr_3C_2 is strongly influenced by pressure and temperature, though pressure exerts a far greater effect on phase formation and purity. Temperature-assisted milling showed only partial conversion, even with extended milling times up to 9 hours, indicating that this temperature range is insufficient to drive complete solid-state diffusion and reaction in the Cr–C system. To further test the effect of mechanical energy alone, additional experiments were performed using a planetary mill without applying pressure. However, even after 64 hours of milling, only chromium peaks were detected, indicating that mechanical energy alone could not overcome the activation barrier. In contrast, the E_{max} mill enables carbide formation even at ambient conditions. Introducing external pressure had a pronounced effect on phase formation: milling at10 bar for 32 hours produced Cr_3C_2 with minor Cr_7C_3 impurities, while extending the duration to 48 hours at the same pressure resulted in phase-pure Cr_3C_2. Higher pressures above 20 bar promoted additional carbide phases, suggesting that moderate pressure offers the most favourable conditions for selective and complete Cr_3C_2 formation. Electrical conductivity measurements showed that powders synthesized at 20 bar exhibited nearly identical contact resistance to those annealed at 800 °C, indicating that the enhanced synthesis efficiency does not compromise the functional properties of the material, making it suitable for applications like fuel cell fillers. These results highlight the potential for pressure-optimised mechanochemical synthesis to serve as an energy-efficient and environmentally-conscious alternative to conventional high-temperature methods, also beyond the synthesis of chromium carbide. One of the key challenges for industrial implementation remains the elimination of the annealing step, which is still required in many mechanochemical routes. Pressurized milling, however, offers a promising approach to overcome this limitation and could serve as a powerful tool to enhance mechanochemical transformations.

Author contributions

ÖA conceived the idea and managed the project. MK designed and performed the experiments, analyzed data, and drafted the manuscript. MK and ÖA discussed the results and reviewed the manuscript.

Conflicts of interest

A patent application on the subject of this study has been filed. MechSyn GmbH, a spin-off from the Max-Planck-Institut für Kohlenforschung, is dedicated to scaling up this process for large-scale production, alongside the development of other high-performance materials.

Data availability

The data supporting this article are provided in the supplementary information (SI). The SI includes details on the thermal and pressure-induced synthesis setups, and the analytical and conductivity data referenced in the main text. Supplementary information is available. See DOI: https://doi.org/10.1039/d5mr00152h.

Acknowledgements

The authors would like to thank the workshops led by D. Ullner and N. Theyssen for their continuous support in maintaining the ball milling devices in good condition. The authors also express their gratitude to the group of C. Weidenthaler for performing the XPS measurements and the group of C. Lehmann for the scanning electron microscopy images and bulk EDX measurements. This project was funded by the EXIST-Forschungstransfer program of the German Federal Ministry for Economic Affairs and Climate Action (BMWK) and Max-Planck-Institute für Kohlenforschung for providing the research facilities.

References

1 S. T. Oyama, *The Chemistry of Transition Metal Carbides and Nitrides*, Springer Netherlands, Dordrecht, 1996.
2 M. Lei, H. Z. Zhao, H. Yang, B. Song and W. H. Tang, Synthesis of transition metal carbide nanoparticles through melamine and metal oxides, *J. Eur. Ceram. Soc.*, 2008, **28**, 1671–1677.
3 S. Ahmad, I. Ashraf, M. A. Mansoor, S. Rizwan and M. Iqbal, An Overview of Recent Advances in the Synthesis and Applications of the Transition Metal Carbide Nanomaterials, *Nanomaterials*, 2021, **11**(3), 776.
4 L. Toth, *Transition Metal Carbides and Nitrides*, Elsevier, 2014.
5 N. Q. Wu, G.-X. Wang, J. M. Wu, Z. Z. Li and M. Y. Yuan, Investigation of TiC formation during ball-milling of elemental titanium and carbon, *Int. J. Refract. Met. Hard Mater.*, 1997, **15**, 289–293.
6 P. Povalyaev, A. Pak, E. Frantsina, Y. Y. Petrova and V. V. Egorova, *Synthesis of Chromium Carbide Powder by Vacuum-free Electric Arc Plasma Method*, 2023.
7 O. M. Cintho, E. A. P. Favilla and J. D. T. Capocchi, Mechanical–thermal synthesis of chromium carbides, *J. Alloys Compd.*, 2007, **439**, 189–195.
8 N. Anacleto and O. Ostrovski, Solid-state reduction of chromium oxide by methane-containing gas, *Metall. Mater. Trans. B*, 2004, **35**, 609–615.
9 M. Mahajan, S. Rajpoot and O. P. Pandey, In-situ synthesis of chromium carbide (Cr3C2) nanopowders by chemical-reduction route, *Int. J. Refract. Met. Hard Mater.*, 2015, **50**, 113–119.
10 S. A. Rasaki, B. Zhang, K. Anbalgam, T. Thomas and M. Yang, Synthesis and application of nano-structured metal nitrides and carbides: A review, *Prog. Solid State Chem.*, 2018, **50**, 1–15.
11 A. Kumar, K. Singh and O. P. Pandey, Direct conversion of wolframite ore to tungsten carbide nano particles, *Int. J. Refract. Met. Hard Mater.*, 2011, **29**, 555–558.

12 O. Ostrovski, G. Zhang, R. Kononov, M. Dewan and J. Li, Carbothermal Solid State Reduction of Stable Metal Oxides, *Steel Res. Int.*, 2010, **81**, 841–846.
13 S. T. Oyama, in *The Chemistry of Transition Metal Carbides and Nitrides*, ed. S. T. Oyama, Springer Netherlands, Dordrecht, 1996, pp. 1–27.
14 G.-G. Lee and B.-K. Kim, Effect of Raw Material Characteristics on the Carbothermal Reduction of Titanium Dioxide, *Mater. Trans.*, 2003, **44**, 2145–2150.
15 G. Zhang and O. Ostrovski, Reduction of titania by methane-hydrogen-argon gas mixture, *Metall. Mater. Trans. B*, 2000, **31**, 129–139.
16 L. Takacs, The historical development of mechanochemistry, *Chem. Soc. Rev.*, 2013, **42**, 7649–7659.
17 S. L. James, C. J. Adams, C. Bolm, D. Braga, P. Collier, T. Friščić, F. Grepioni, K. D. M. Harris, G. Hyett, W. Jones, A. Krebs, J. Mack, L. Maini, A. G. Orpen, I. P. Parkin, W. C. Shearouse, J. W. Steed and D. C. Waddell, Mechanochemistry: opportunities for new and cleaner synthesis, *Chem. Soc. Rev.*, 2012, **41**, 413–447.
18 S. M. Hick, C. Griebel and R. G. Blair, Mechanochemical synthesis of alkaline Earth carbides and intercalation compounds, *Inorg. Chem.*, 2009, **48**, 2333–2338.
19 Z. Zhao, H. Zheng, S. Liu, J. Shen, W. Song and J. Chen, Low temperature synthesis of chromium carbide (Cr3C2) nanopowders by a novel precursor method, *Int. J. Refract. Met. Hard Mater.*, 2015, **48**, 46–50.
20 S. Mateti, M. Mathesh, Z. Liu, T. Tao, T. Ramireddy, A. M. Glushenkov, W. Yang and Y. I. Chen, Mechanochemistry: A force in disguise and conditional effects towards chemical reactions, *Chem. Commun.*, 2021, **57**, 1080–1092.
21 Z. Zhao and W. Hu, Synthesis and characterization of chromium carbide nanopowders processed by mechanical alloying assisted microwave heating route, *Int. J. Refract. Met. Hard Mater.*, 2016, **58**, 206–210.
22 P. Matteazzi and G. Le Caër, Room-Temperature Mechanosynthesis of Carbides by Grinding of Elemental Powders, *J. Am. Ceram. Soc.*, 1991, **74**, 1382–1390.
23 J. Meyers, Ö. Agbaba, H. Buchholz and F. Schüth, Mechanochemically Synthesized Transition Metal Carbide Fillers for Coating Metallic Bipolar Plates in Proton Exchange Membrane Fuel Cells, *Energy Technol.*, 2026, **14**(1), DOI: 10.1002/ente.202501231.
24 S. Gomari and S. Sharafi, Microstructural characterization of nanocrystalline chromium carbides synthesized by high energy ball milling, *J. Alloys Compd.*, 2010, **490**, 26–30.
25 H. Huang and P. G. McCormick, Effect of milling conditions on the synthesis of chromium carbides by mechanical alloying, *J. Alloys Compd.*, 1997, **256**, 258–262.
26 B. L. Jiang, Z. L. Kou, D. J. Ma, Y. K. Wang, C. X. Li, W. R. Duan and X. H. Yang, Mechanical Behavior of the Cr_3C_2 Compound at High Pressure and High Temperature, *AMR*, 2015, **1120–1121**, 1187–1193.
27 W. Schmidt, P. Losch, H. Petersen, M. Etter, F. Baum, J. Ternieden and C. Weidenthaler, Pressure as the driving force for mechanochemical reactions on the example of ion metathesis of alkali halides upon ball milling, *RSC Mechanochem.*, 2025, **2**, 273–284.
28 L. D. Teng, K. G. Lu, R. E. Aune and S. Seetharaman, Thermodynamic investigations of Cr3C2 and reassessment of the Cr-C system, *Metall. Mater. Trans. A*, 2004, **35**, 3673–3680.
29 S. Reichle, M. Felderhoff and F. Schüth, Mechanocatalytic Room-Temperature Synthesis of Ammonia from Its Elements Down to Atmospheric Pressure, *Angew. Chem., Int. Ed. Engl.*, 2021, **60**, 26385–26389.
30 N. Fairley, V. Fernandez, M. Richard-Plouet, C. Guillot-Deudon, J. Walton, E. Smith, D. Flahaut, M. Greiner, M. Biesinger, S. Tougaard, D. Morgan and J. Baltrusaitis, Systematic and collaborative approach to problem solving using X-ray photoelectron spectroscopy, *Appl. Surf. Sci. Adv.*, 2021, **5**, 100112.
31 Y. Zou, D. He, X. Wei, R. Yu, T. Lu, X. Chang, S. Wang and L. Lei, Nanosintering mechanism of MgAl2O4 transparent ceramics under high pressure, *Mater. Chem. Phys.*, 2010, **123**, 529–533.
32 C. Suryanarayana, Mechanical alloying and milling, *Prog. Mater. Sci.*, 2001, **46**, 1–184.
33 G. Dercz, I. Matuła, J. Maszybrocka, M. Zubko, J. Barczyk, L. Pająk and S. Stach, Effect of milling time and presence of Sn on the microstructure and porosity of sintered Ti-10Ta-8Mo and Ti-10Ta-8Mo-3Sn alloys, *J. Alloys Compd.*, 2019, **791**, 232–247.
34 M. Trautmann, H. Ahmad and G. Wagner, Influencing the Size and Shape of High-Energy Ball Milled Particle Reinforced Aluminum Alloy Powder, *Materials*, 2022, **15**(9), 3022.
35 D. Gouvêa, Thermodynamic of solid-state sintering: Contributions of grain boundary energy, *J. Eur. Ceram. Soc.*, 2024, **44**, 116677.
36 F. Zheng, L. Wang, R. Wang, J. Wang, S. Zhang, Q. Hu and L. Wang, The Pore Microstructure Evolution and Porous Properties of Large Capillary Pressure Wicks Sintered with Carbonyl Nickel Powder, *Materials*, 2022, **15**(17), 5830.
37 L. Sun, X. Ji, L. Zhao, W. Zhai, L. Xu, H. Dong, Y. Liu and J. Peng, First Principles Investigation of Binary Chromium Carbides Cr7C3, Cr3C2 and Cr23C6: Electronic Structures, Mechanical Pro erties and Thermodynamic Properties under Pressure, *Materials*, 2022, **15**(2), 558.
38 B. Deng, Z. Wang, W. Chen, J. T. Li, D. X. Luong, R. A. Carter, G. Gao, B. I. Yakobson, Y. Zhao and J. M. Tour, Phase controlled synthesis of transition metal carbide nanocrystals by ultrafast flash Joule heating, *Nat. Commun.*, 2022, **13**, 262.
39 T. M. Vidyuk, A. V. Ukhina, A. I. Gavrilov, V. S. Shikalov, A. G. Anisimov, O. I. Lomovsky and D. V. Dudina, Synthesis of Tungsten Carbides in a Copper Matrix by Spark Plasma Sintering: Microstructure Formation Mechanisms and Properties of the Consolidated Materials, *Materials*, 2023, **16**(15), 5385.

